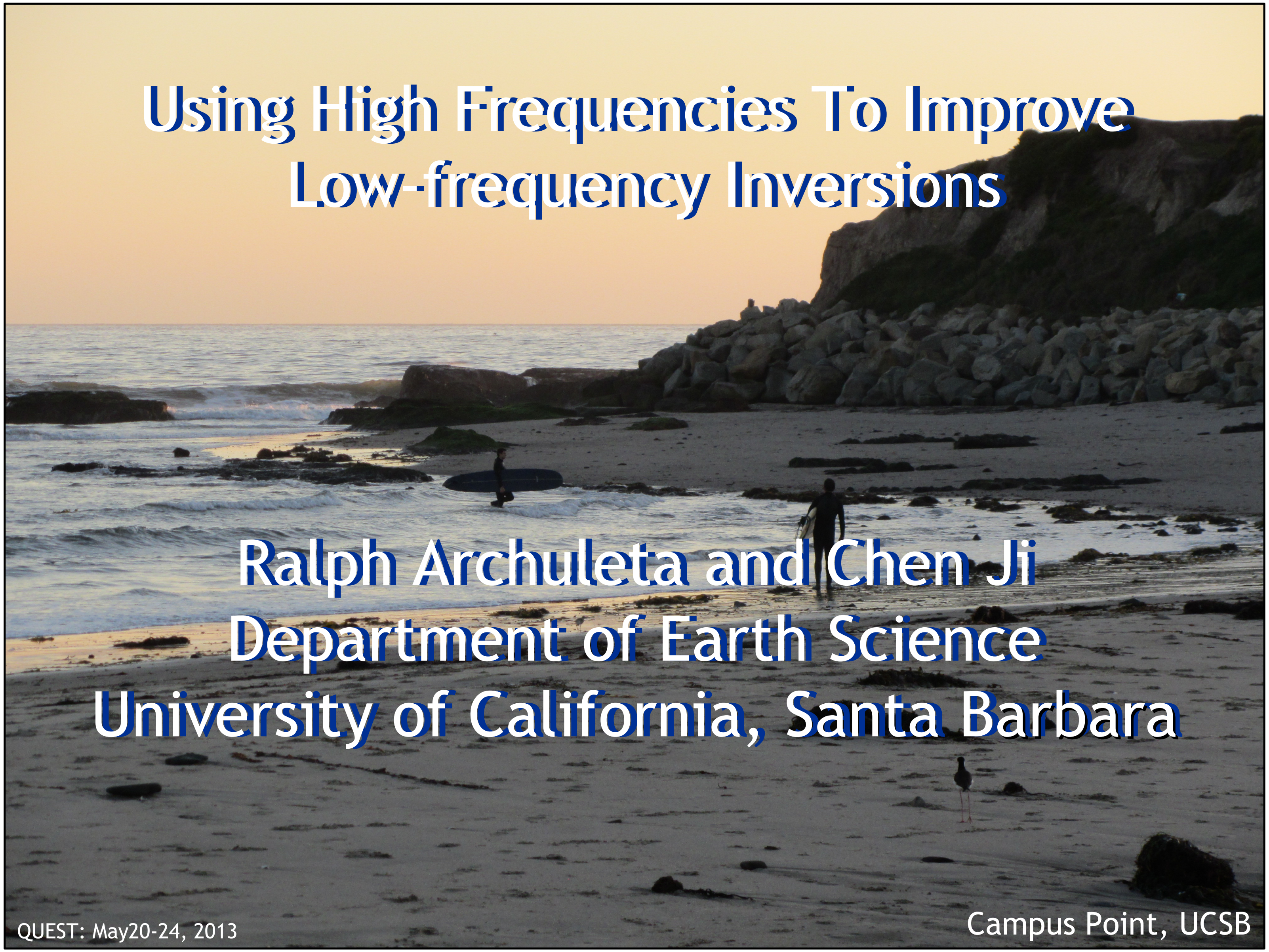

Using High Frequencies To Improve
Low-frequency Inversions
Ralph Archuleta and Chen Ji
Department of Earth Science
University of California, Santa Barbara
QUEST: May20-24, 2013
Campus Point, UCSB

Describing the Earthquakes Source: Kinematics

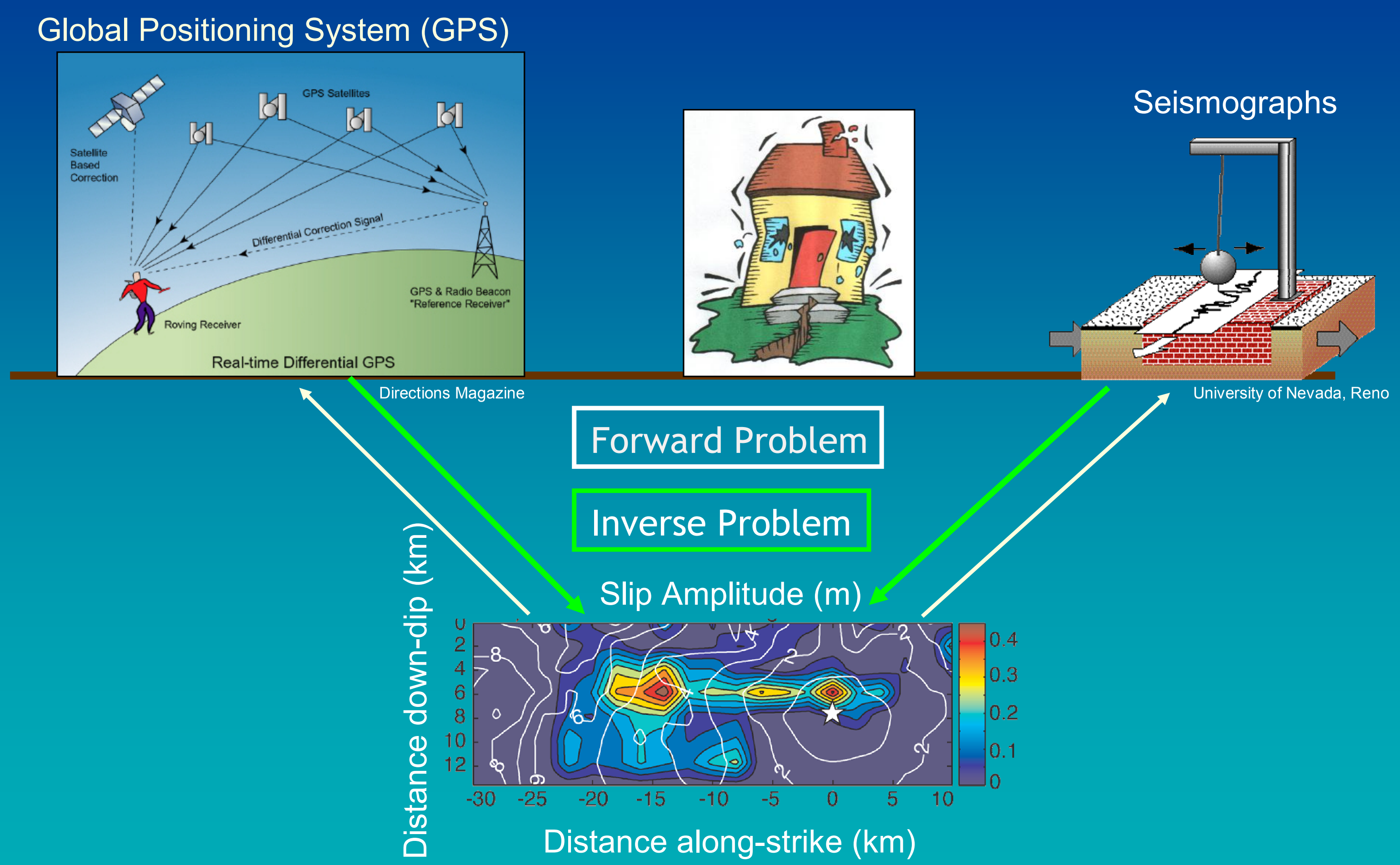

QUEST: May20-24, 2013

Courtesy of S. Custódio

Source Representation (Ji et al., 2002, 2003)

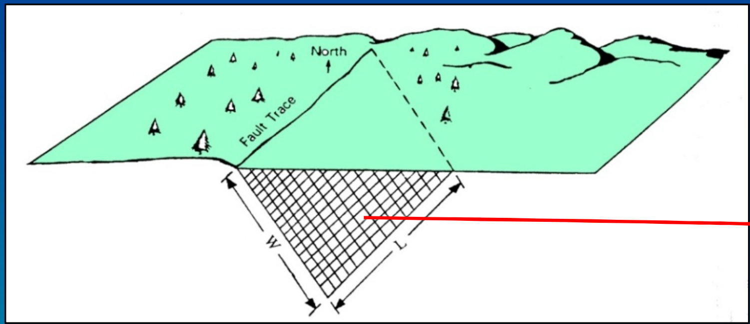

$$Y^i_{jk}(t,t',\vec{x}) = \sum_p G^i_{jk}(\vec{x}'_p,\vec{x},t) * \delta(t - \Delta t^p_{jk} - t')$$

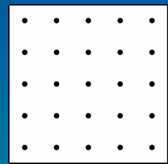

$$\vec{u}(t,\vec{x}) = \int_{-\infty}^{\infty} d\tau \iint_{\Sigma} [u_i(\xi,\tau)] c_{ijpq} \partial G_{np}(\vec{x}, t-\tau; \xi, 0)/\partial \xi_q \, d\Sigma$$

$$\vec{u}(t,\vec{x}) \approx \sum_{j=1}^{n}\sum_{k=1}^{m} D_{jk}[\cos(\lambda_{jk}) Y^1_{jk}(t,t',\vec{x}) + \sin(\lambda_{jk}) Y^2_{jk}(t,t',\vec{x})] * \dot{S}_{jk}(t)$$

D_{jk}	Slip amplitude
λ_{jk}	Rake angle
$\dot{S}_{jk}(t)$	Derivative rise time function
t'	Rupture initiation time
$Y^i_{jk}(t,t',\vec{x})$	Subfault Green's functions

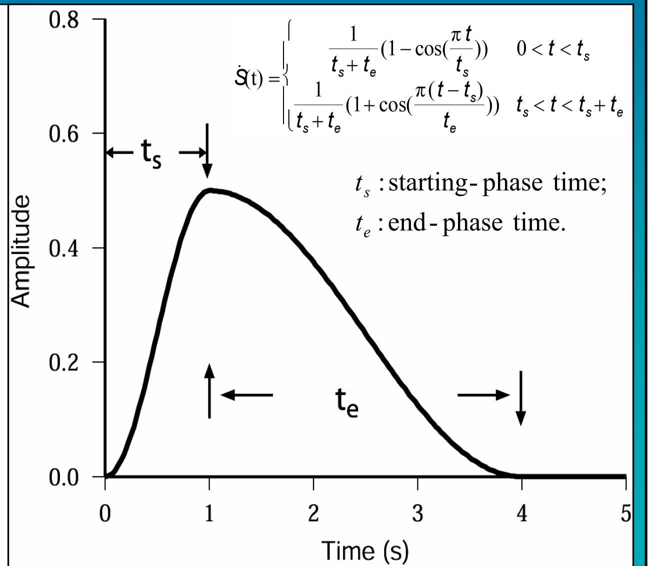

Rise time function *S(t)*

Aki-Brune Acceleration Spectrum

GPS Inversion Seismic Inversion

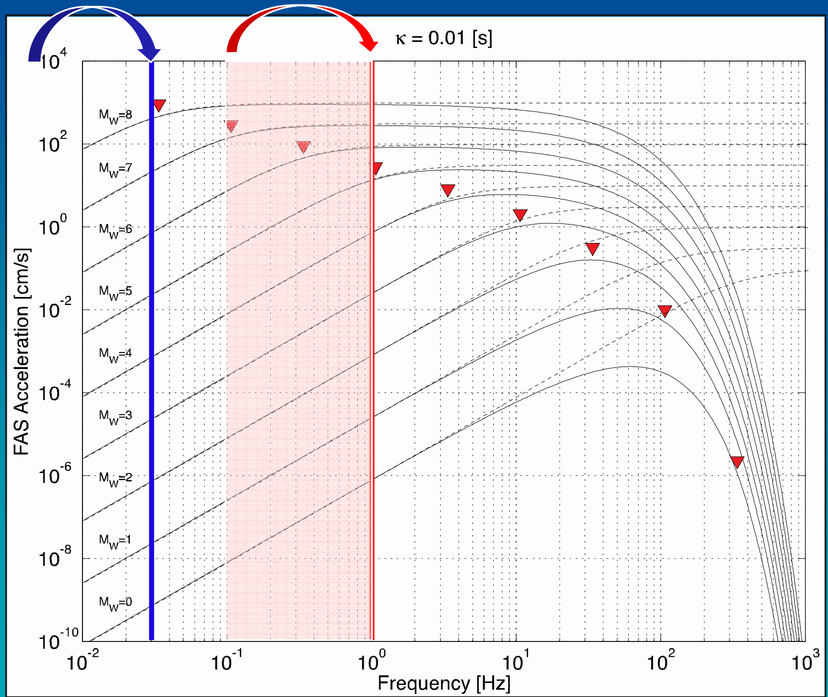

Corner Frequency for Δσ=5 MPa

Displacement Spectrum

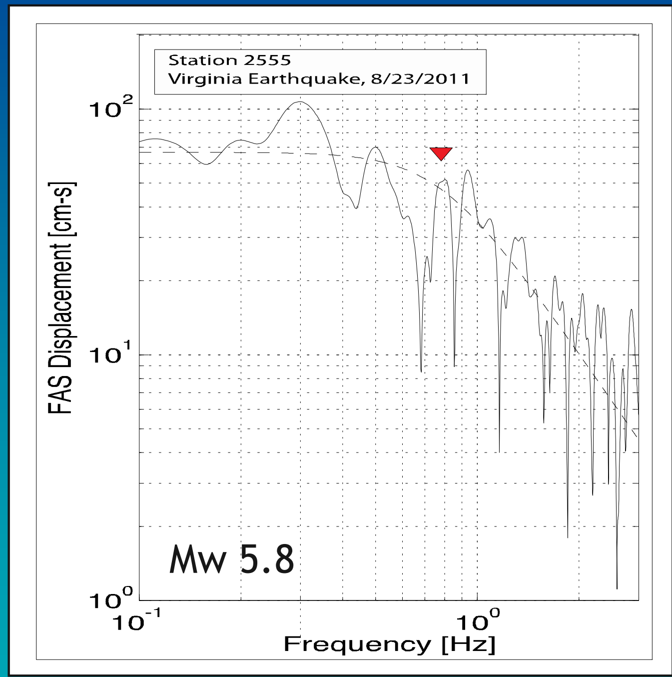

Energy in Aki-Brune Spectrum

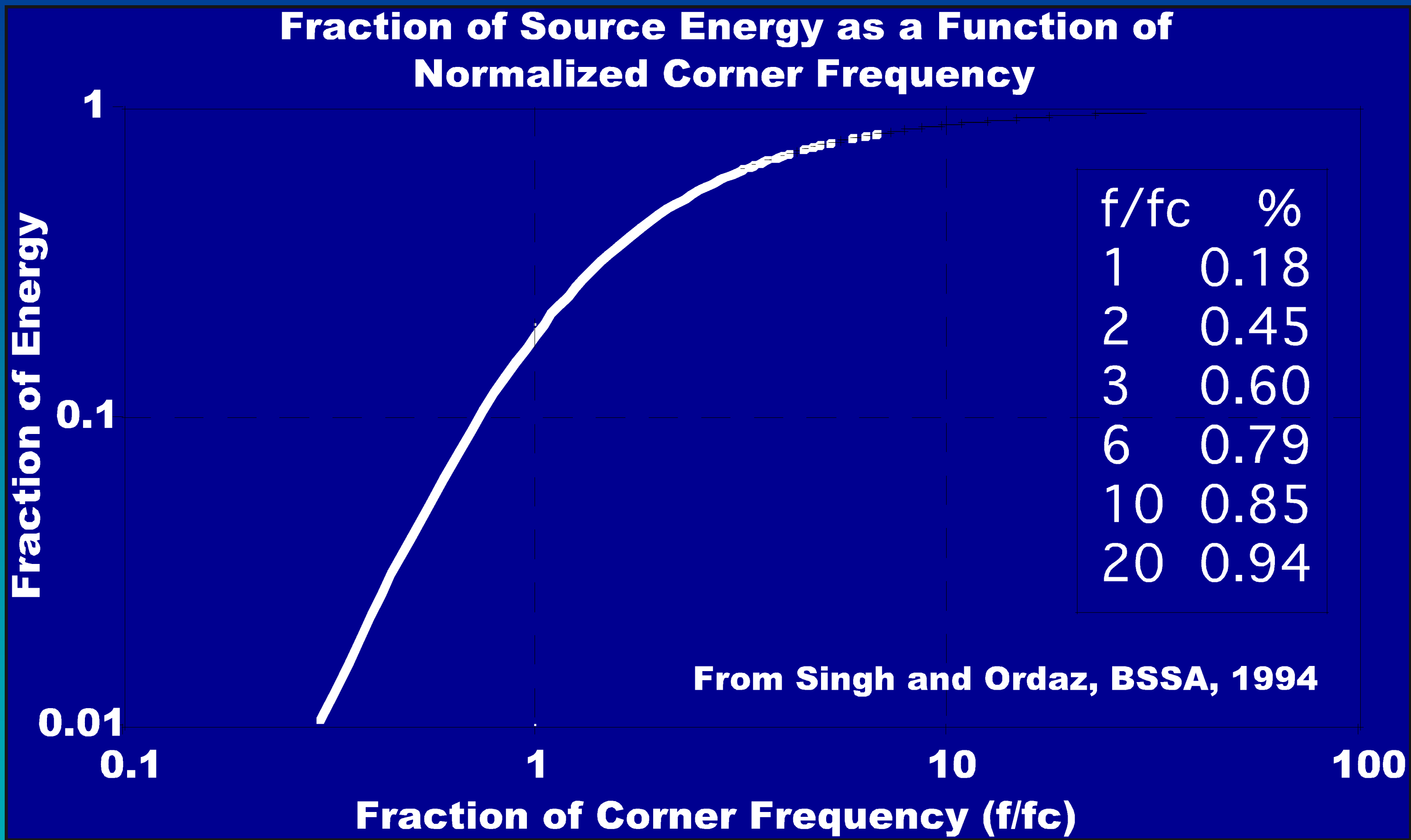

Energy Is Concentrated Near the Corner Frequency

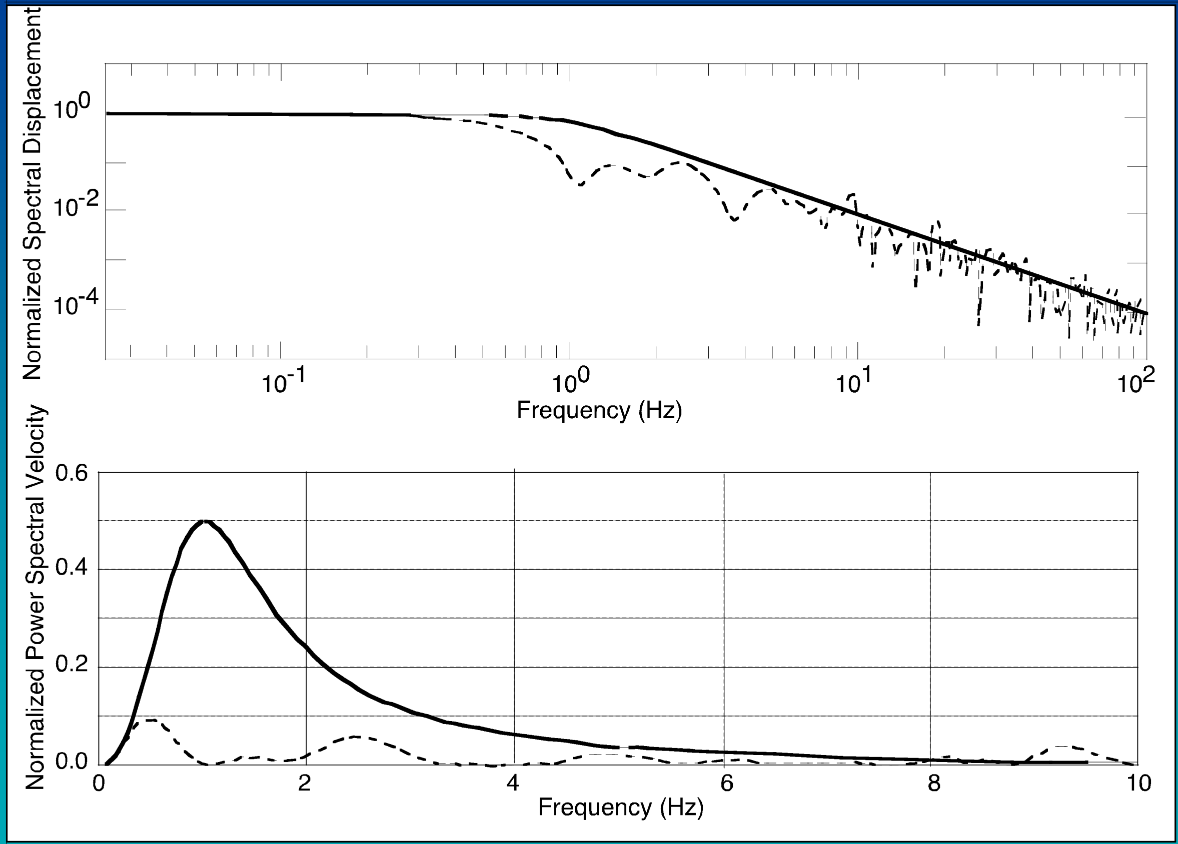

Tumarkin & Archuleta, 1994

Parkfield Earthquake, M_w 6.0
September 28, 2004

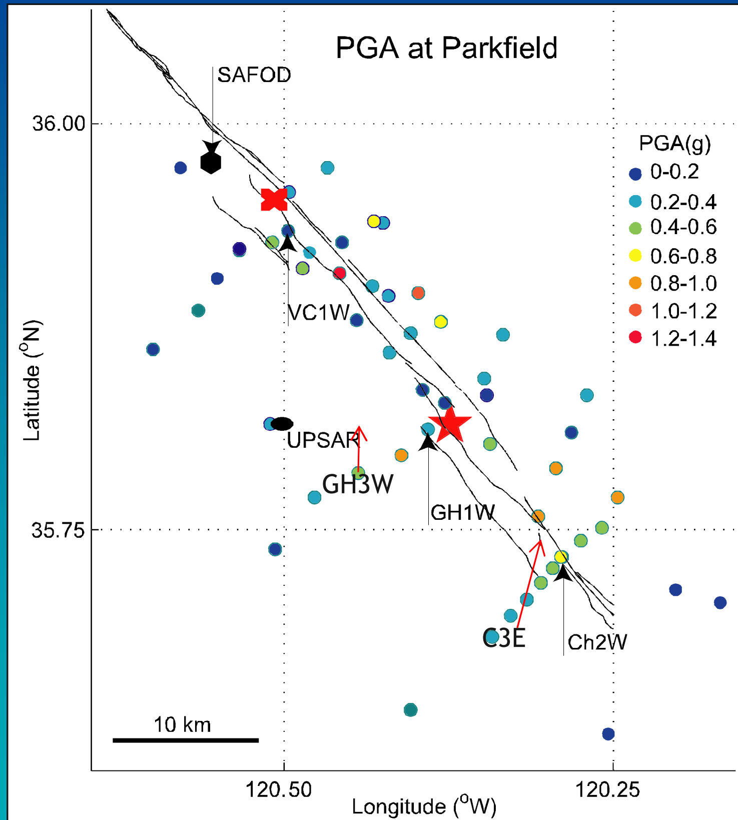

Spectrograms: Station C3E & GH3W

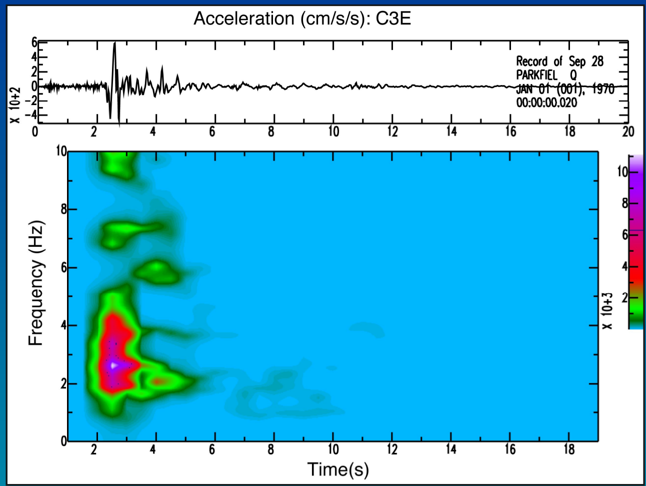

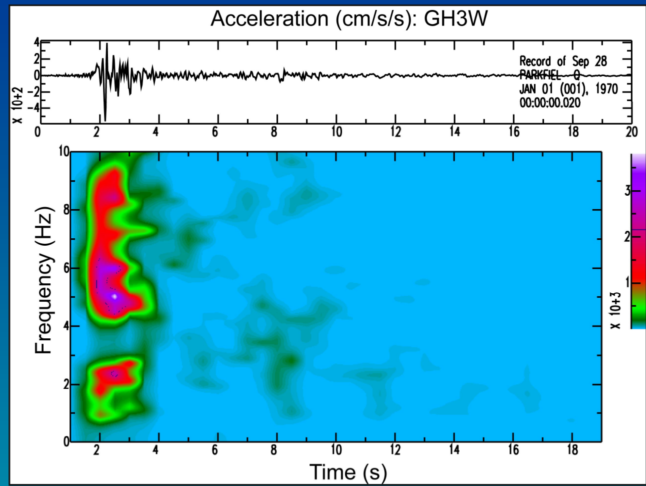

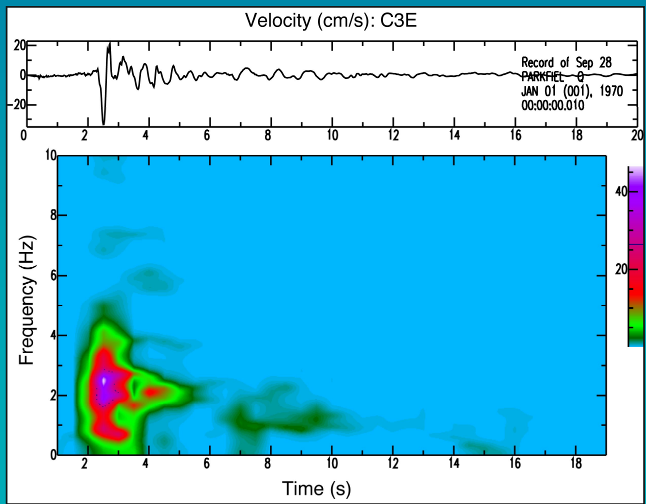

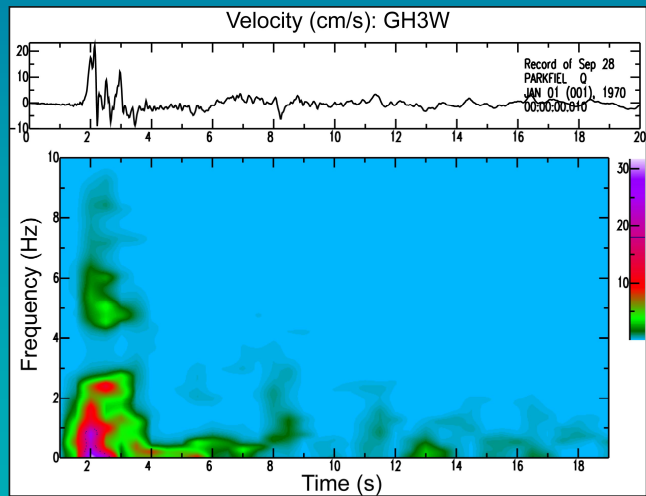

Courtesy of S. Custódio

Frequency at which Ground Motion Is Coherent

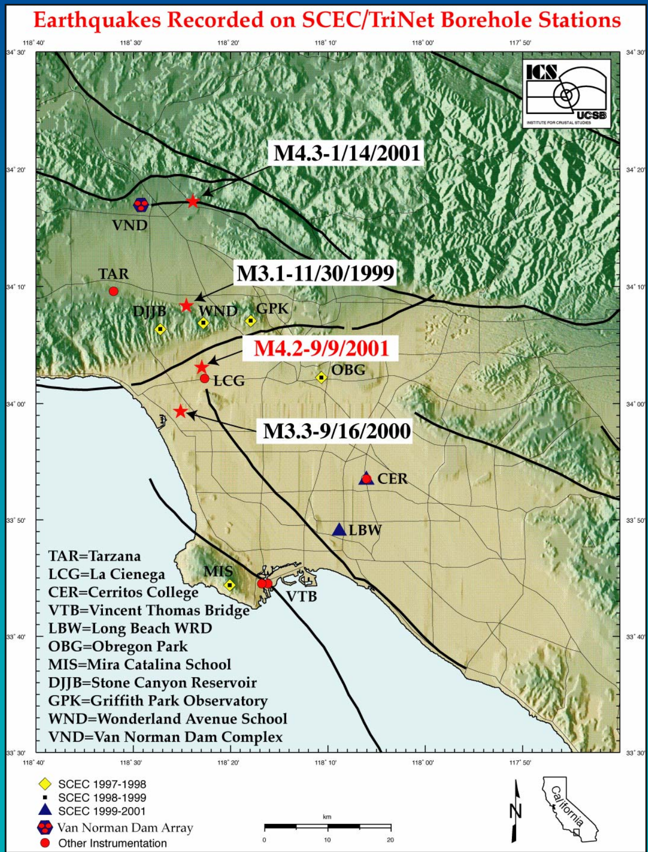

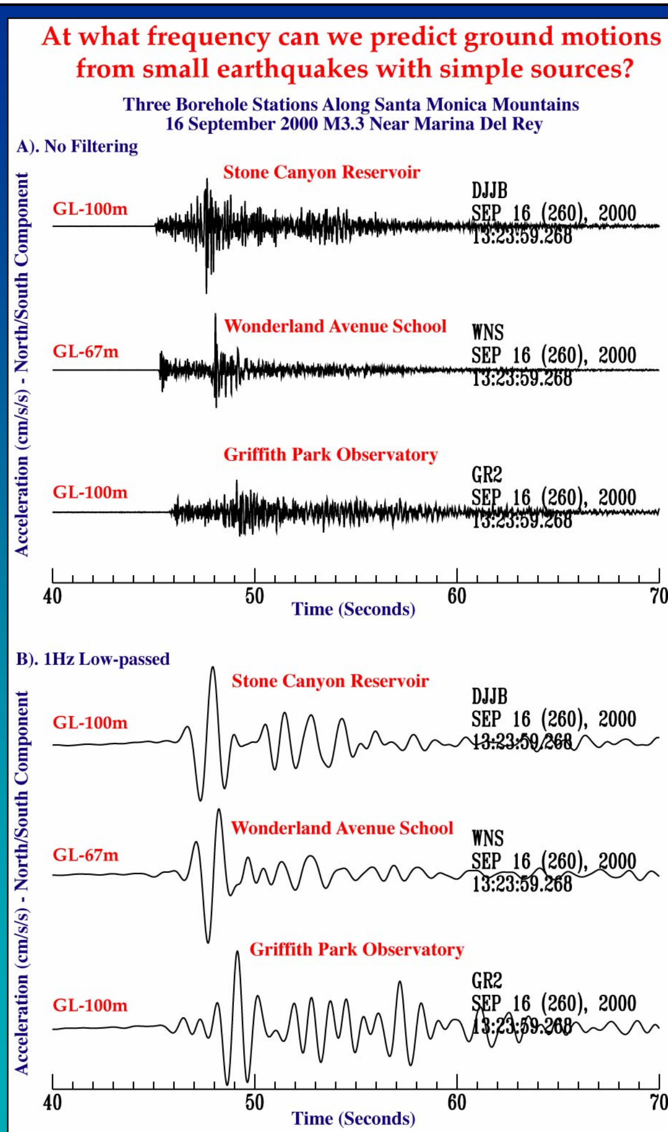

QUEST: May20-24, 2013

Courtesy of Jamie Steidl

SPICE BlindTest I (Mai et al., 2007)

- **Data**
  1: Seismic data in velocity (*fmax* ~ 3 Hz)
  2: Static displacements
- **Available information**
  1: Fault geometry & Hypocentral location (strike, dip, rake: 150°, 90°, 0°)
  2: Total seismic moment: 1.43×10^{26} dyne-cm
  3: Velocity structure
  4: Rupture does not break the surface
- **To be resolved:**
  1. Slip distribution on the fault plane
  2. Rupture velocity & rise time (both are constant; the investigators were given this information but not the values)

Input model

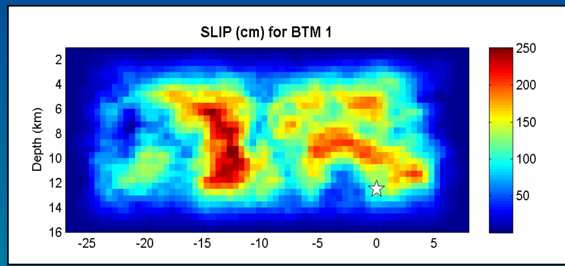

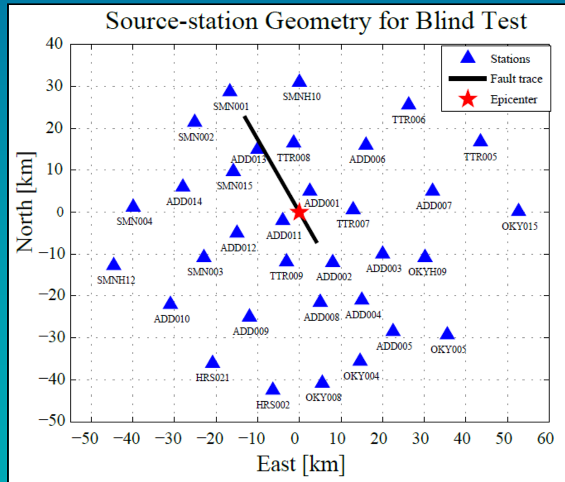

BlindTest website: http://www.seismo.ethz.ch/staff/martin/BlindTest.html

Spectrum: Energy Ratio

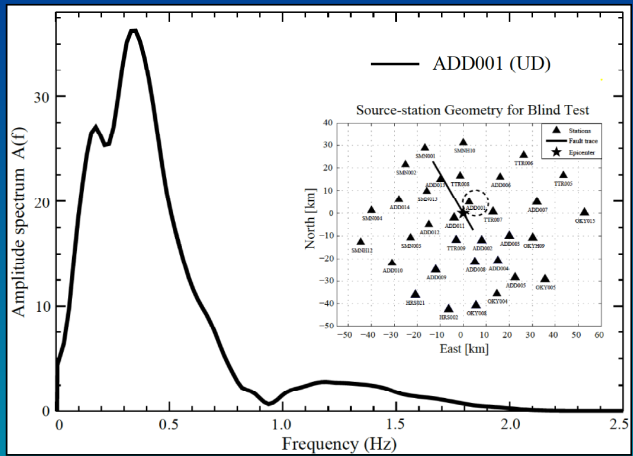

Average relative energy

$$\overline{R}^b = \frac{100}{N}\sum_{i=1}^{N}\frac{\int (o_i^b(t))^2 dt}{\int (o_i(t))^2 dt}$$

Relative Energy			
0-2.0 (Hz)	*0-0.1 (Hz)*	*0.1-1.0 (Hz)*	*1.0-2.0 (Hz)*
100%	15.04%	86.02%	2.73%

Note:

Misfit functions, such as variance reduction, are designed to catch the difference in amplitude (or energy). Therefore, for this case, it is dominated by the signals from 0.1 to 1 Hz.

Shao & Ji, GJI 2012

Forward Calculation

Vertical components in velocity

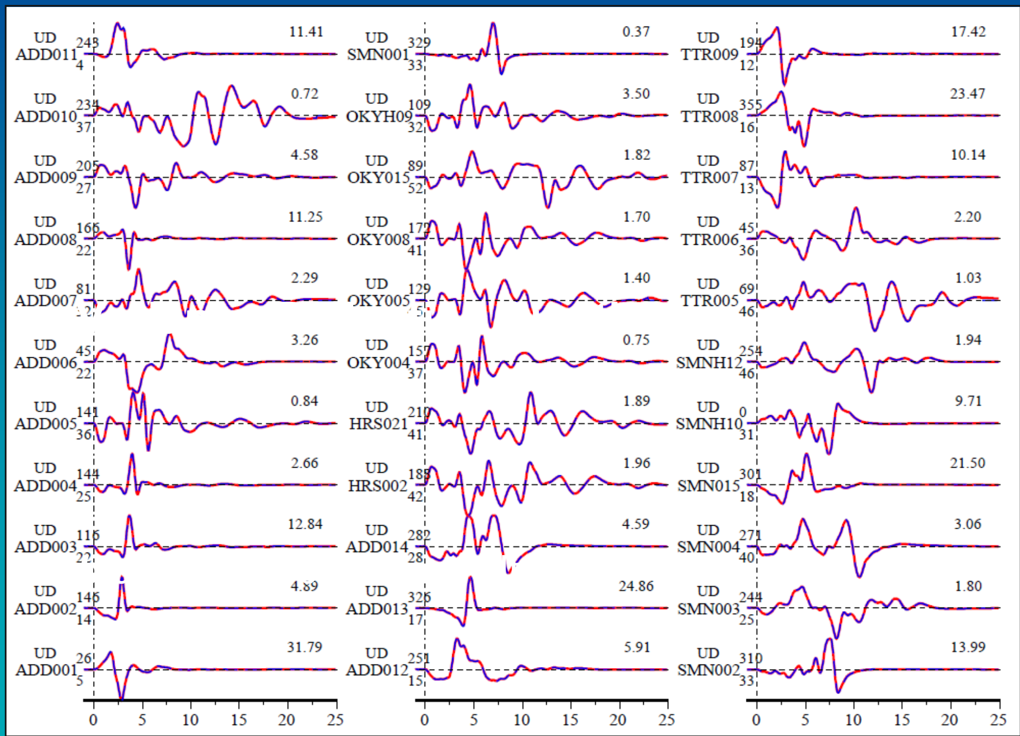

Indistinguishable visually !

Input model

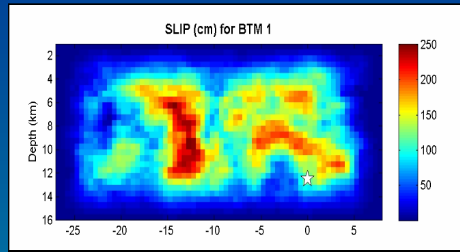

Corrected data

Double of our synthetics

Target

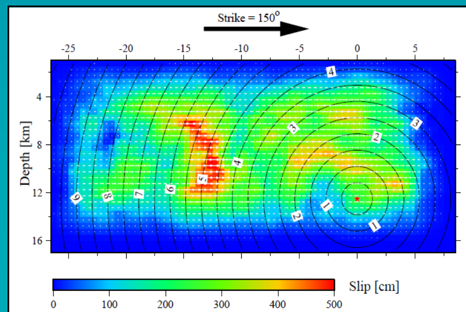

Shao & Ji, GJI 2012

Variance Reduction

Variance Reduction Function

$$\overline{V}^b = \frac{1}{N}\sum_{i=1}^{N}\frac{\int (o_i^b(t) - s_i^b(t))^2 dt}{\int (o_i^b(t))^2 dt}$$

b denotes a bandpass filter

Variance reductions			
0-2.0 (Hz)	*0-0.1 (Hz)*	*0.1-1.0 (Hz)*	*1.0-2.0 (Hz)*
99.91%	**99.98%**	**99.92%**	**97.53%**

Shao & Ji, GJI 2012

Variance Reduction: 3 Models

Target_SC

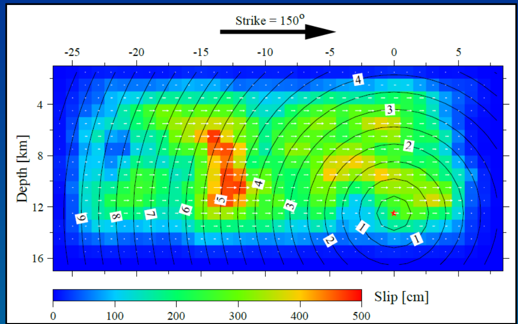

Model I

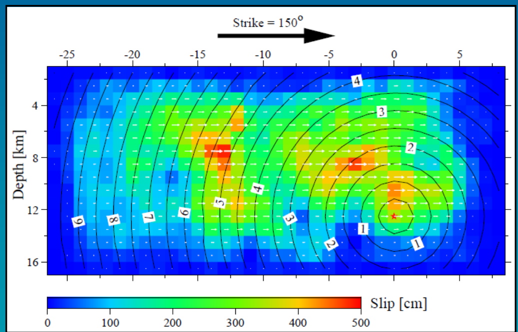

Model III

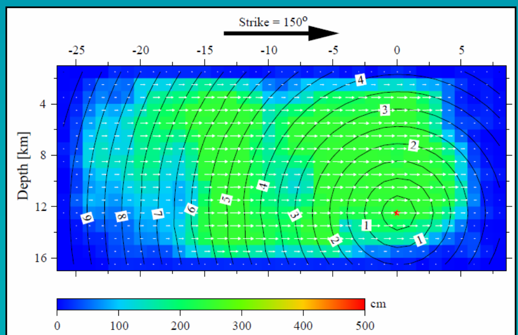

Models	*Variance reductions*			
	0-2.0 (Hz)	*0-0.1 (Hz)*	*0.1-1.0 (Hz)*	*1.0-2.0 (Hz)*
Target_SC	99.32%	99.72%	99.45%	86.21%
Model I	99.35%	99.28%	99.61%	77.02%
Model III	98.87%	98.90%	99.36%	64.26%

Model III cannot match the signals from 1 to 2 Hz.

Shao & Ji, GJI 2012

Sensitivity Test: Peak Slip

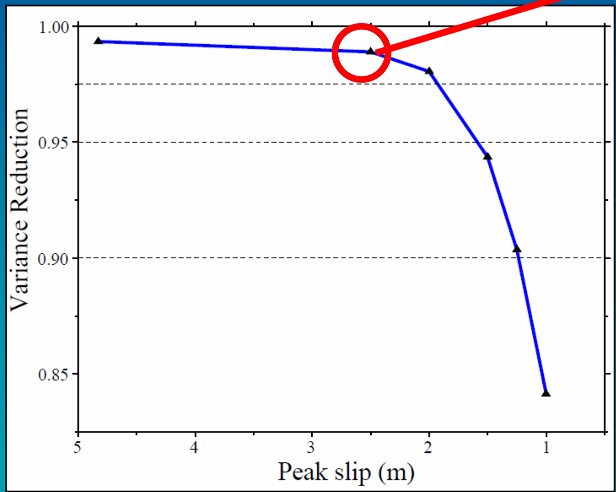

Model III: Peak slip =2.5 m

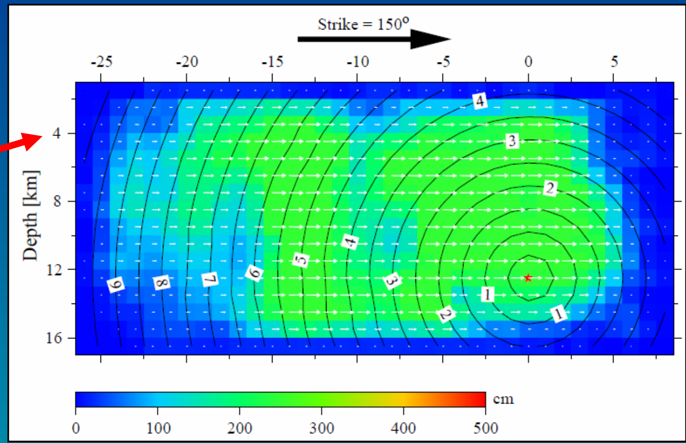

Target_SC

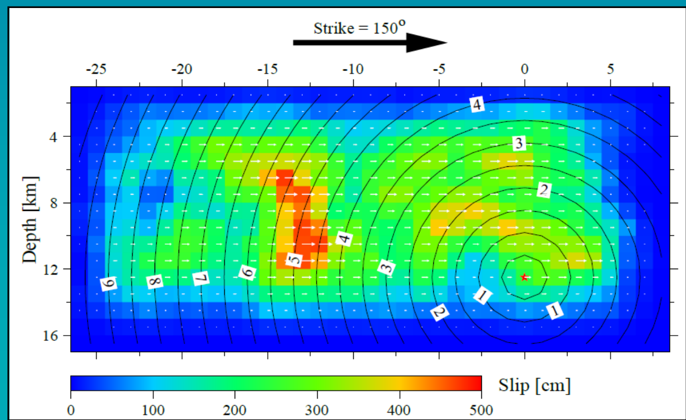

“Coherence” Function

High frequency signals are sensitive to the details of the slip models.

$$e(f) = \frac{1}{N}\left|\sum_{i}^{N} \frac{2REAL[d_i(f)s_i^*(f)]}{d_i(f)d_i^*(f)+s_i(f)s_i^*(f)}\right|$$

Model I

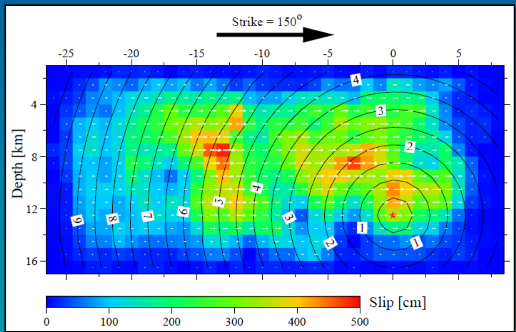

Model III

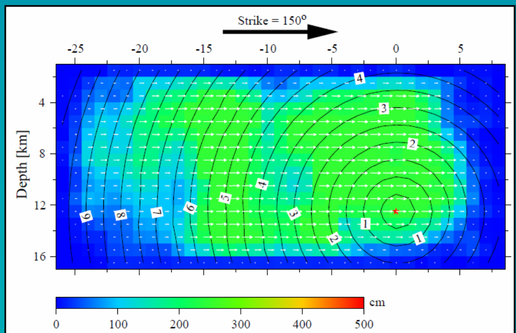

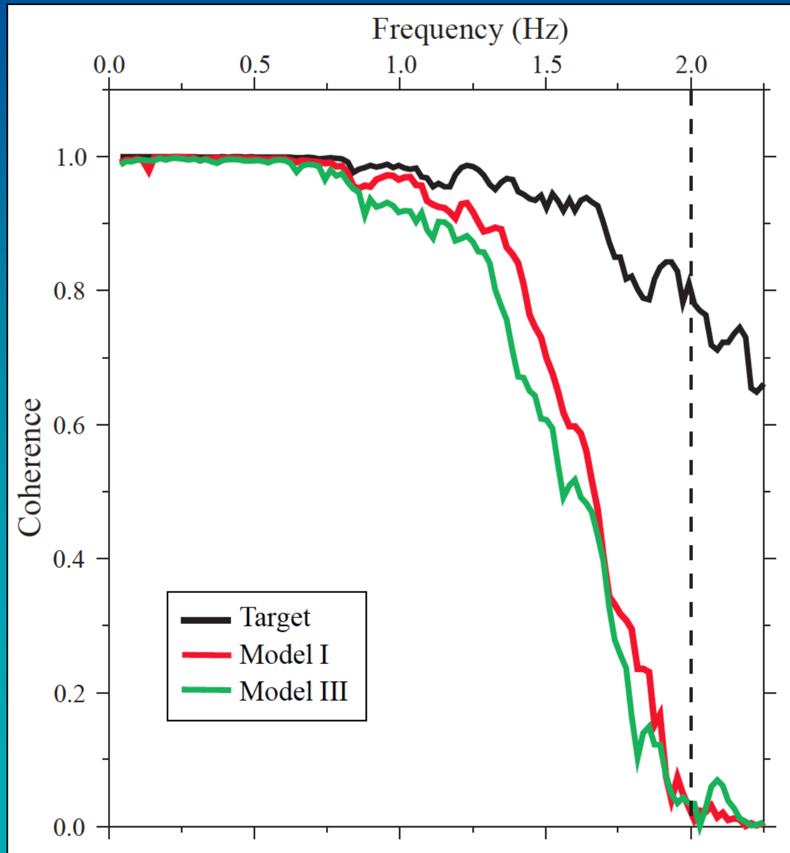

Shao & Ji, GJI 2012

Comparing Moment Rate Functions

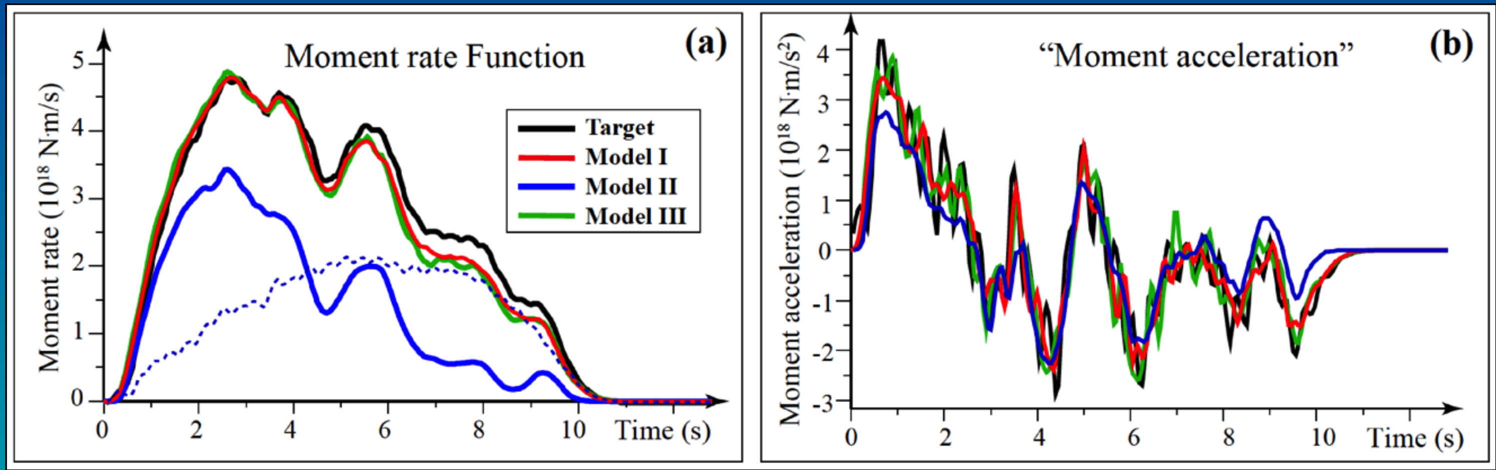

Far field body-wave

1: Displacement

$$U(\vec{r},t) \approx \frac{1}{4\pi\rho\nu^{3}}\psi(\theta,\phi)\frac{1}{r}\dot{M}(t)$$

2: Velocity

$$V(\vec{r},t) \approx \frac{1}{4\pi\rho\nu^{3}}\psi(\theta,\phi)\frac{1}{r}\ddot{M}(t)$$

Shao & Ji, GJI 2012

Back-projection

L stations

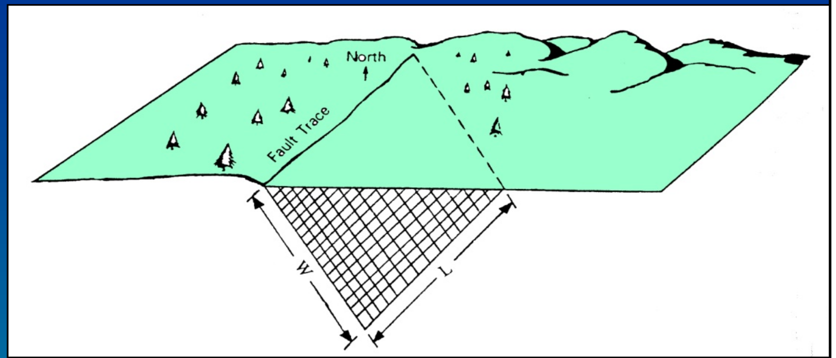

Suppose the excited ground motion at the *i-th* station can be repre[sented as]

$$s_i(t) = \sum_{j=1}^{N} \dot{M}_o^j(t) * W_i^j(t)$$

For the j-th subevent, we can define simple back-propagation function (**SBP**) and network response function (**NRF**) as

$$sbp_j(t) = \sum_{i=1}^{L} s_i(t) * W_i^j(-t)$$

$$nrf_j(t) = \sum_{i=1}^{L} W_i^j(t) * W_i^j(-t)$$

$$mbf_j(t) = sbf_j(t) *^{-1} nrf_j(t)$$

Modified back-projection function (**MBF**)

It is straightforward to prove

$$mbf_j(t) = \dot{M}_0^j(t) + \sum_{k \neq j}^{N} \dot{M}_0^k(t) * \left[\sum_{i=1}^{L} W_i^k(t) * W_i^j(-t) \right] *^{-1} nrf_j(t)$$

Target

Imaging error caused by the slip on the rest of fault plane

[Yano et al., in preparation]

Slip rate function

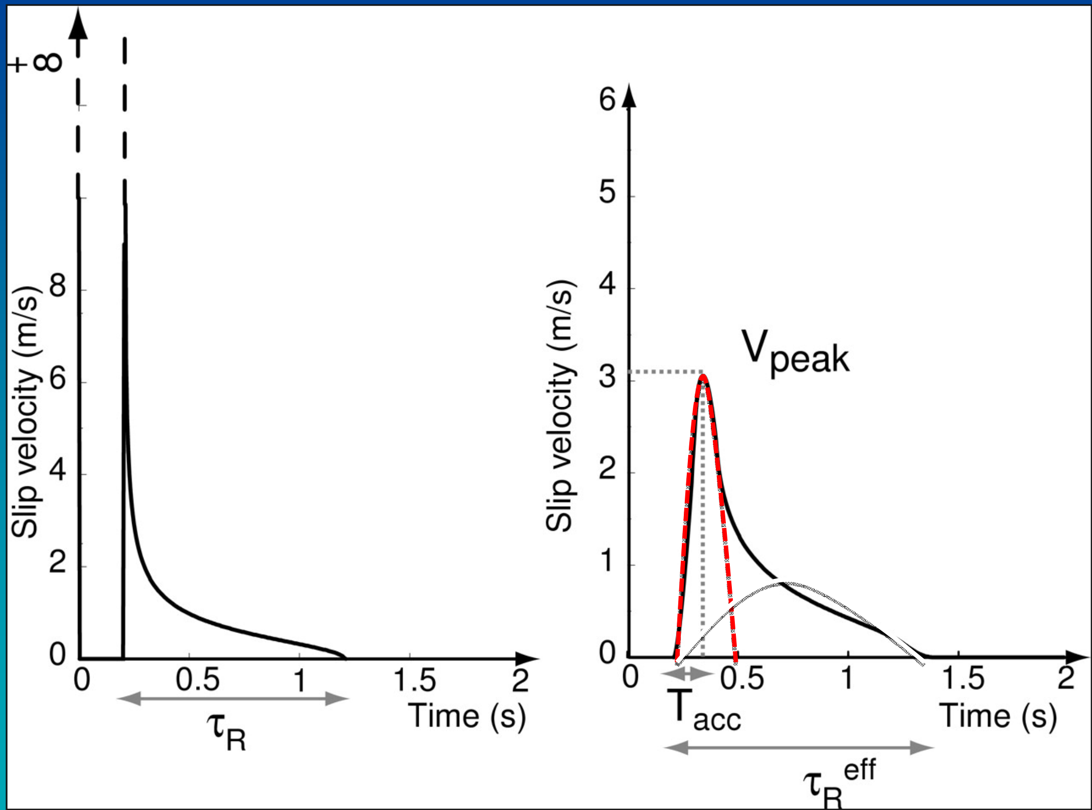

As the high frequency radiation is mainly caused by the initial rupture, we assume the target subevent has a 0.8 s triangular slip rate function.

[Tinti et al., 2005]

Comparison of Back-projection Functions and Network Response Function

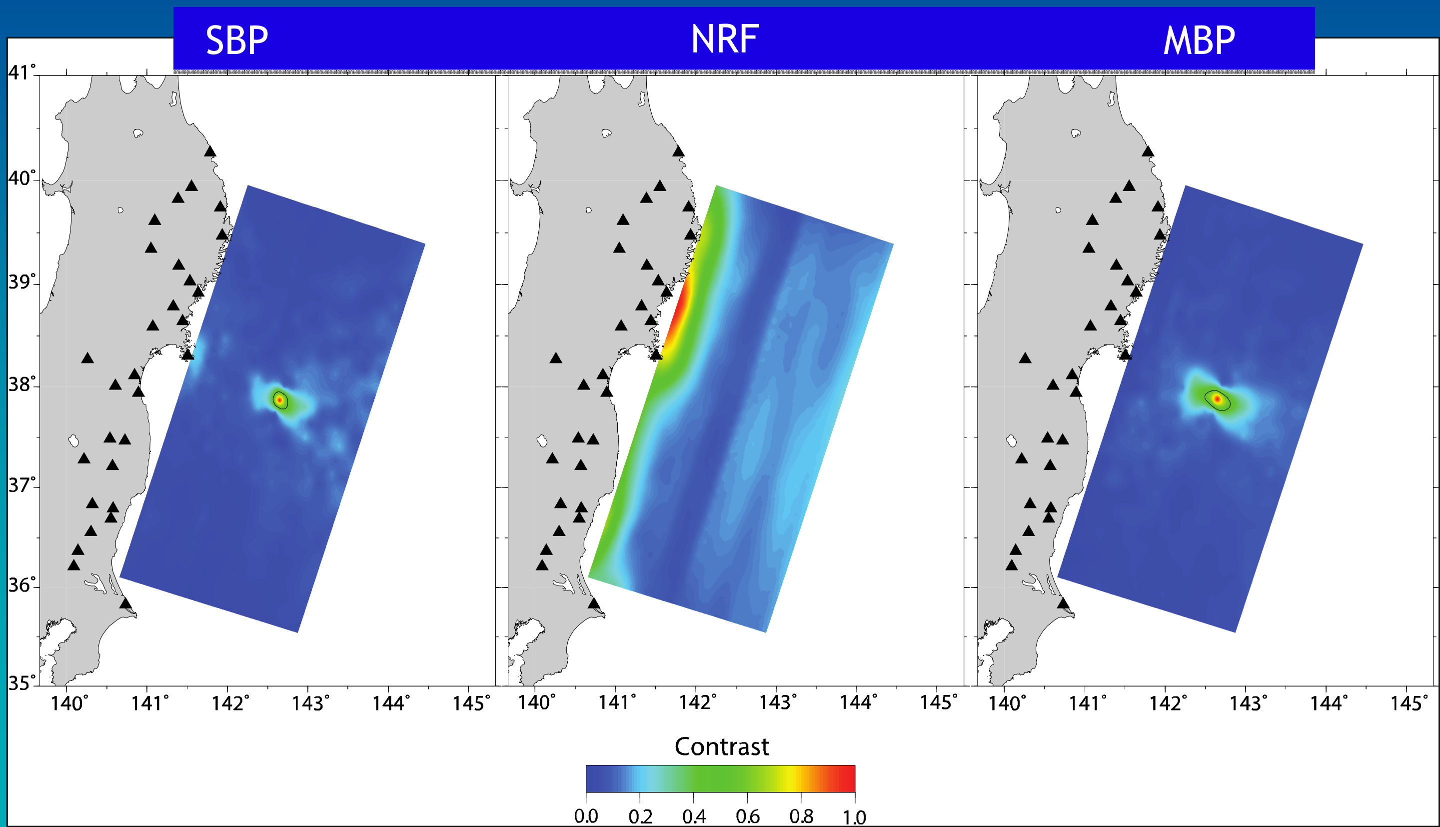

[Yano, 2012]

Numerical Test: Effect of Station Distribution

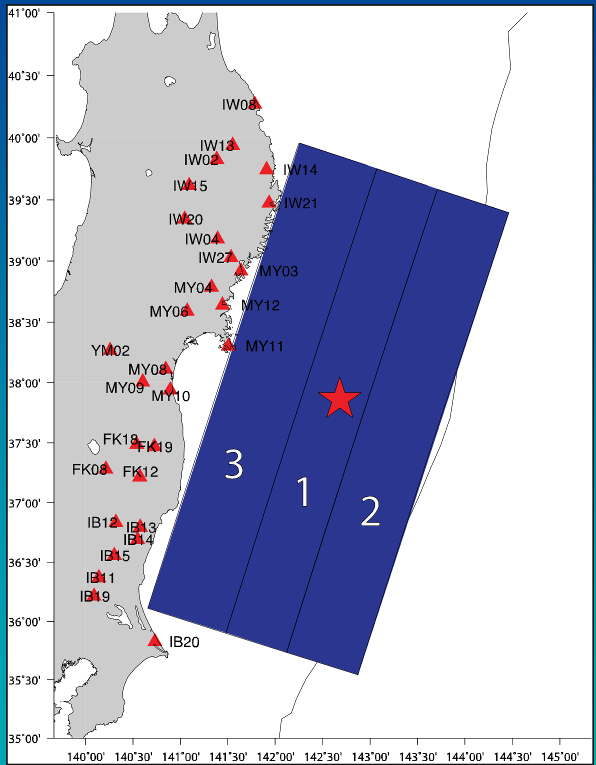

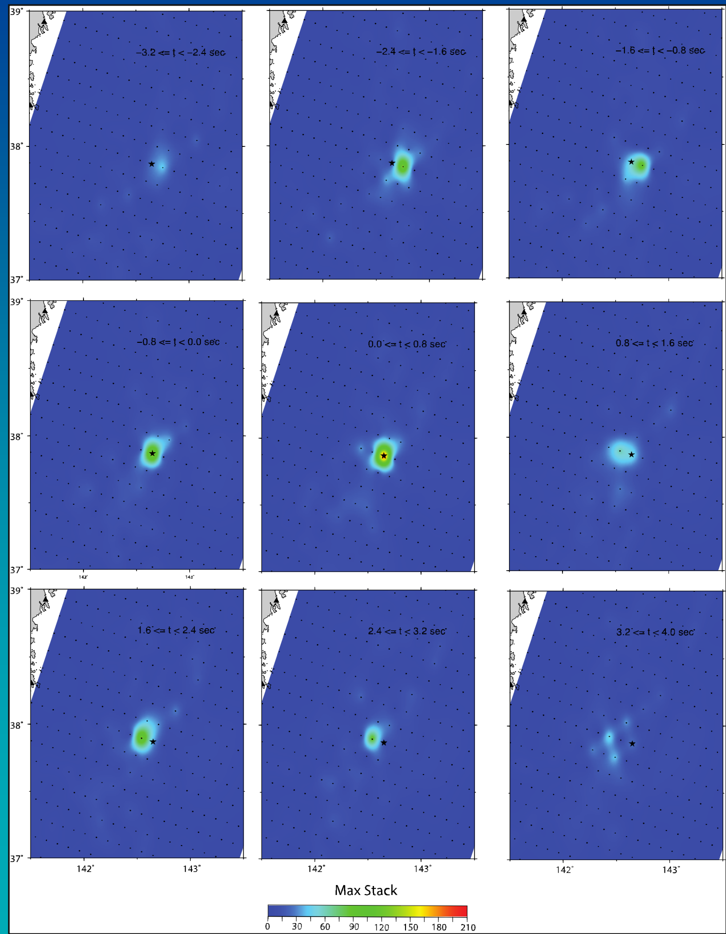

[Yano, 2012]

Numerical Test

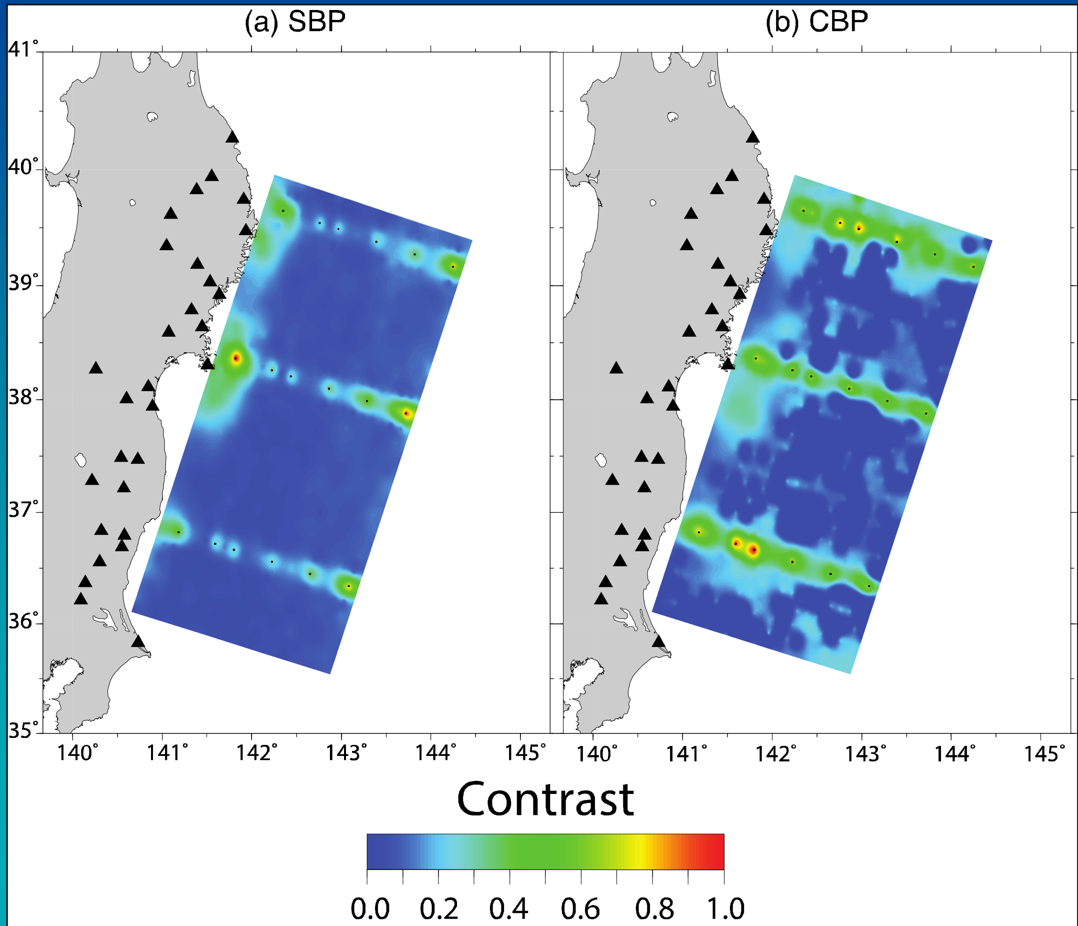

[Yano, 2012]

Back-projection

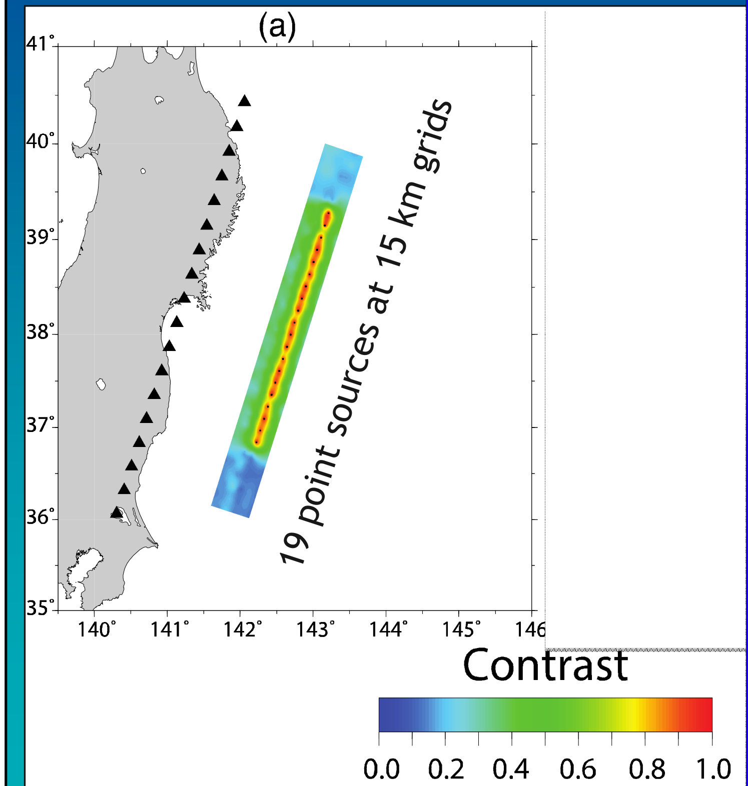

Synthetic Observations:

18 uniformly distributed stations on one side. Such a station distribution has relatively lower spatial resolution in down-dip direction but shall be optimal to track along strike rupture.

Target sources:
19 point sources distribute along a line with 15 km interval. A constant 0.8 s triangular slip rate function. Rupture propagation with a speed of 1.5 km/s.

The data has been bandpass filtered from 0.03 Hz to 1 Hz before this back-propagation analysis

[Yano, 2012]

Back-projection Test Case

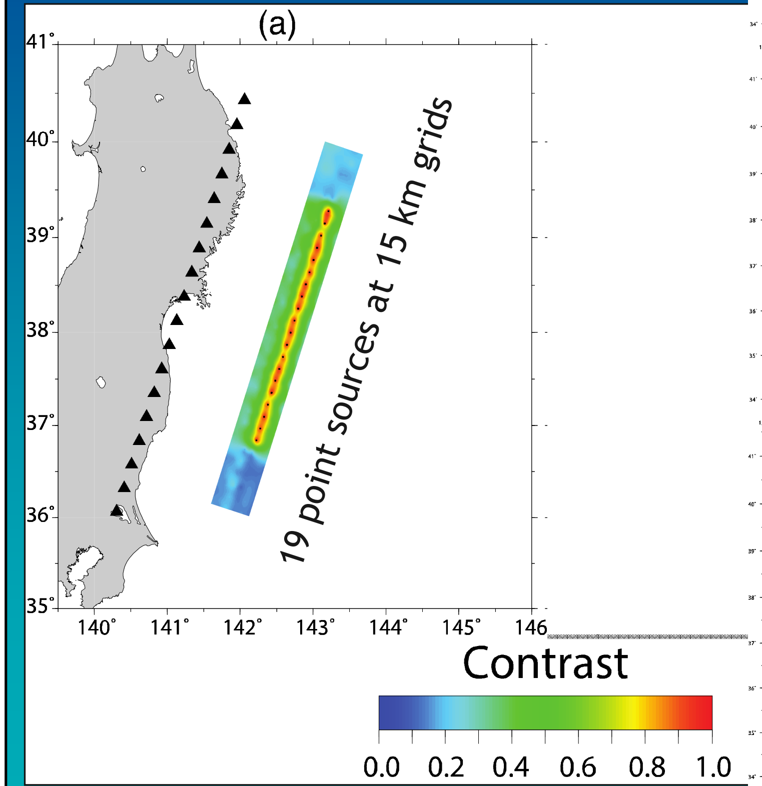

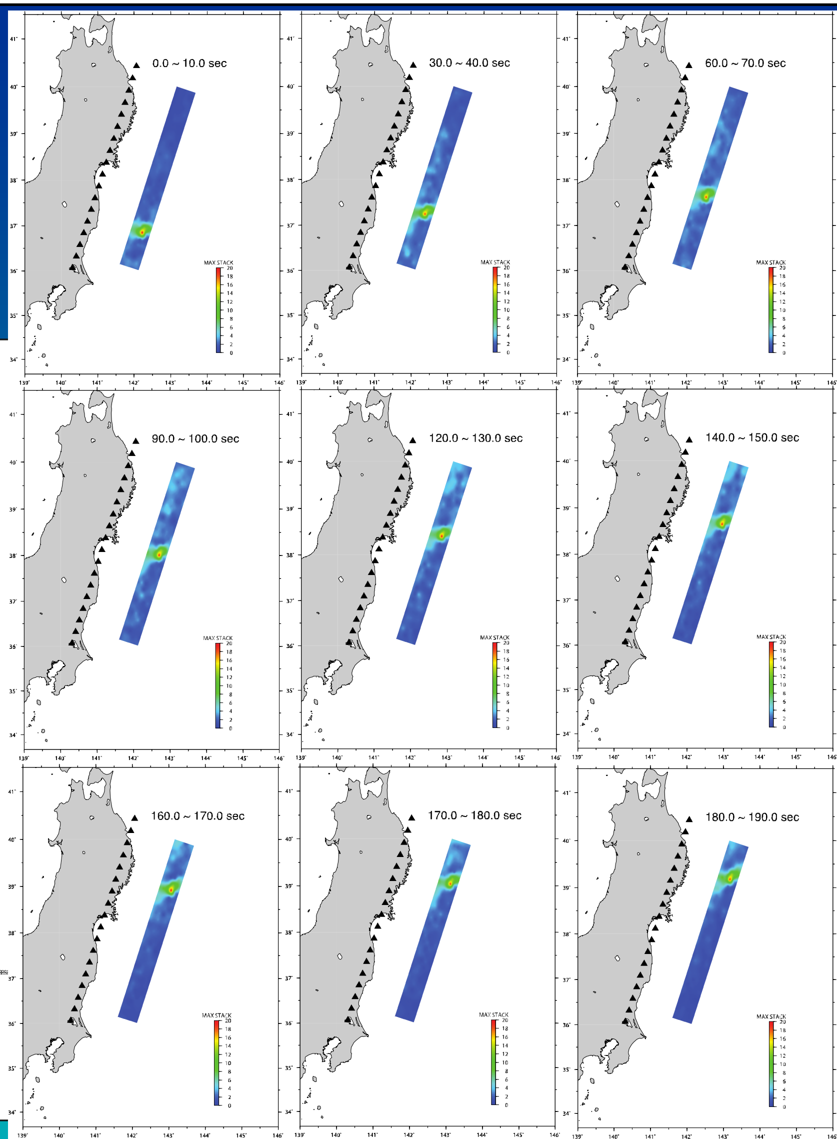

[Yano, 2012]

Back-Projection

[Yano et al., 2012]

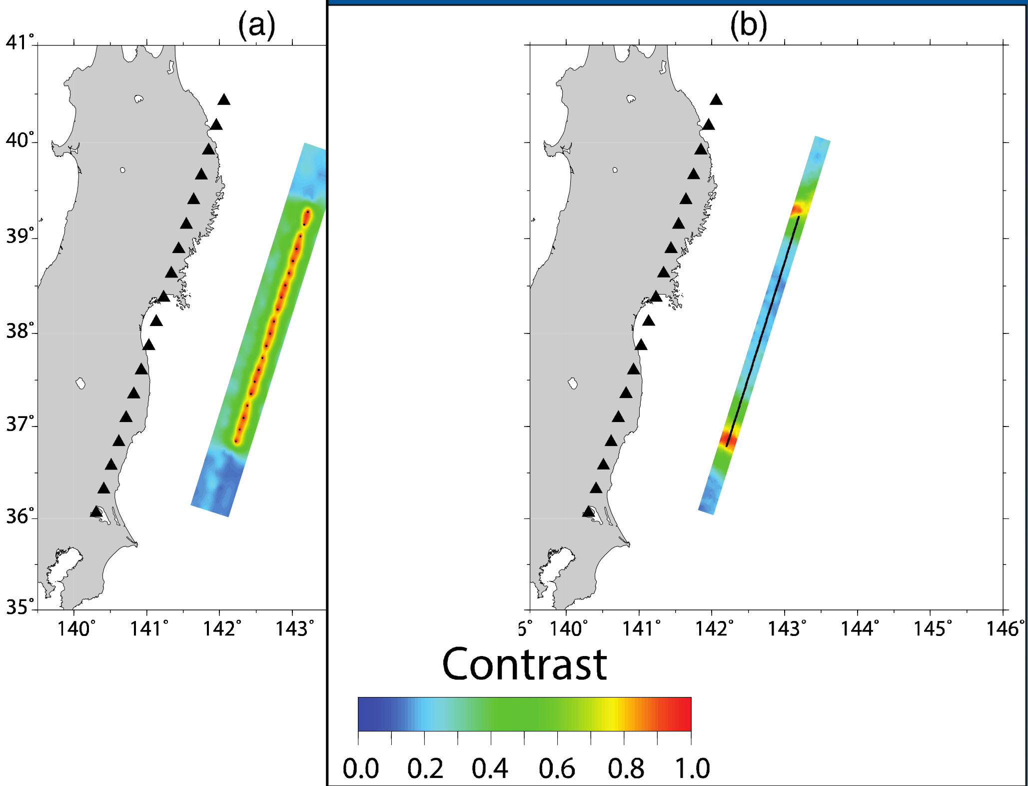

Synthetic Observations:

18 uniformly distributed stations on one side. Such a station distribution has relatively lower spatial resolution in down-dip direction but shall be optimal to track along strike rupture.

Target sources:
270 point sources distribute along a line with 1 km interval. A constant 0.8 s triangular slip rate function. Unilateral rupture with a velocity of 1.5 km/s.

The data has been bandpass filtered from 0.03 Hz to 1 Hz before this back-propagation analysis

[Yano, 2012]

Back-Projection

[Yano et al., 2012]

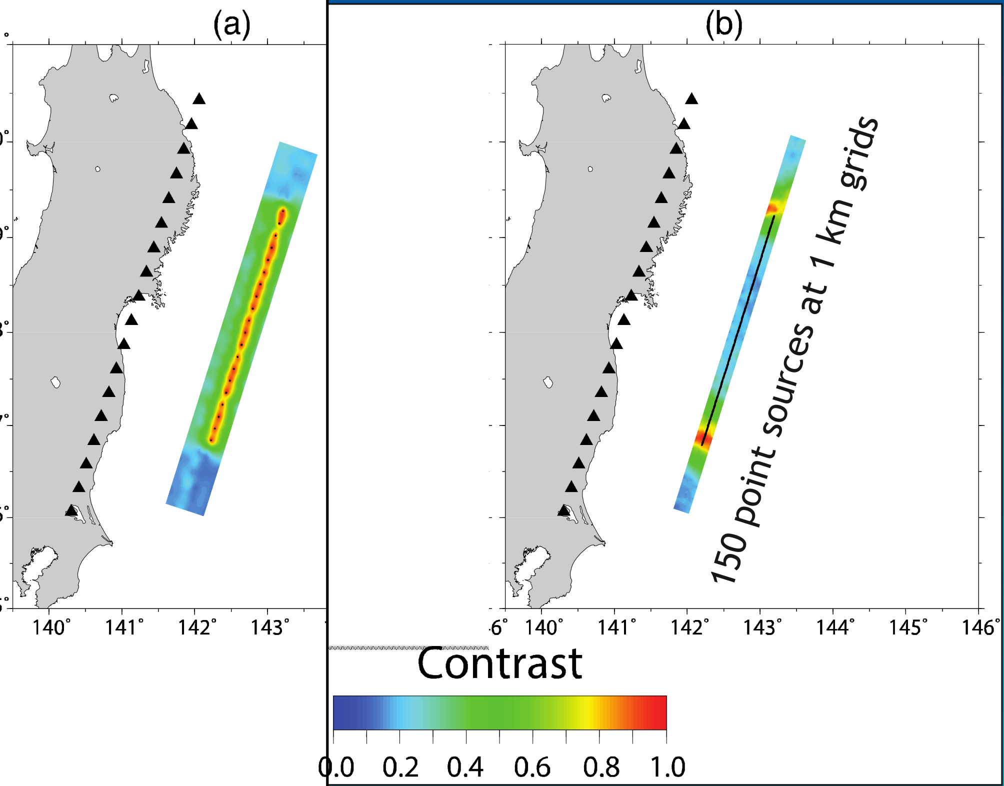

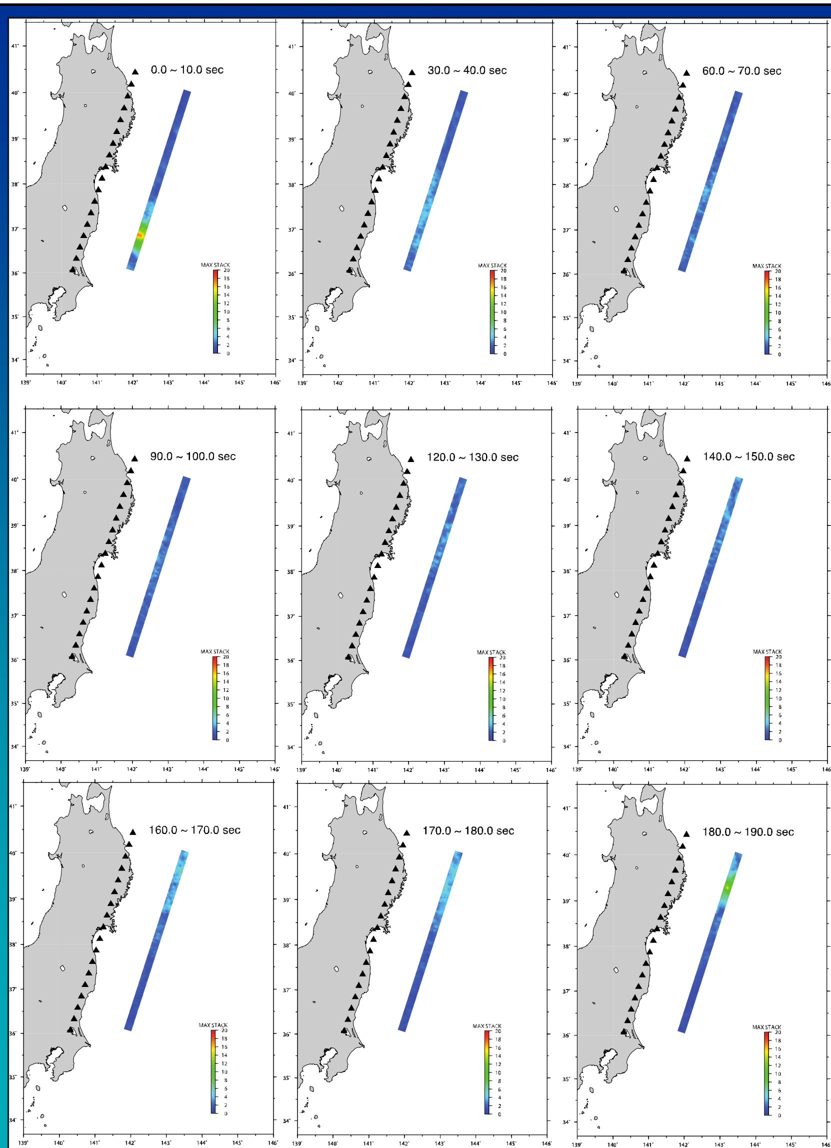

[Yano, 2012]

Comparison of Moment Rate Functions

15 km interval target sources

1 km interval target sources

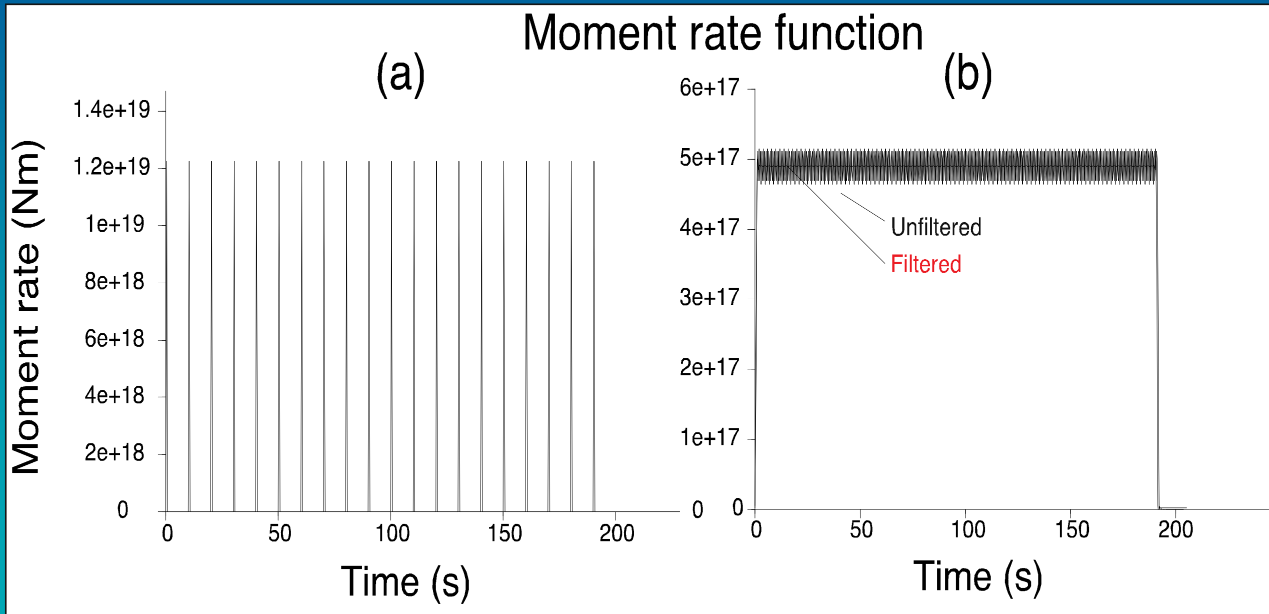

[Yano, 2012]

Target sources at 15 km intervals

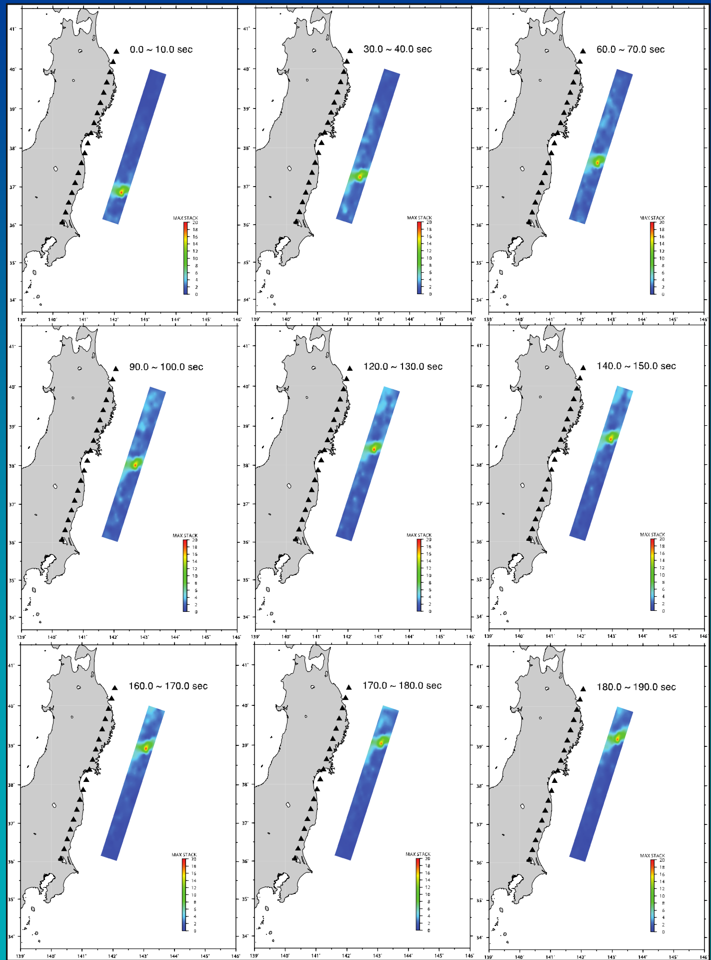

Target sources at 1.0 km intervals

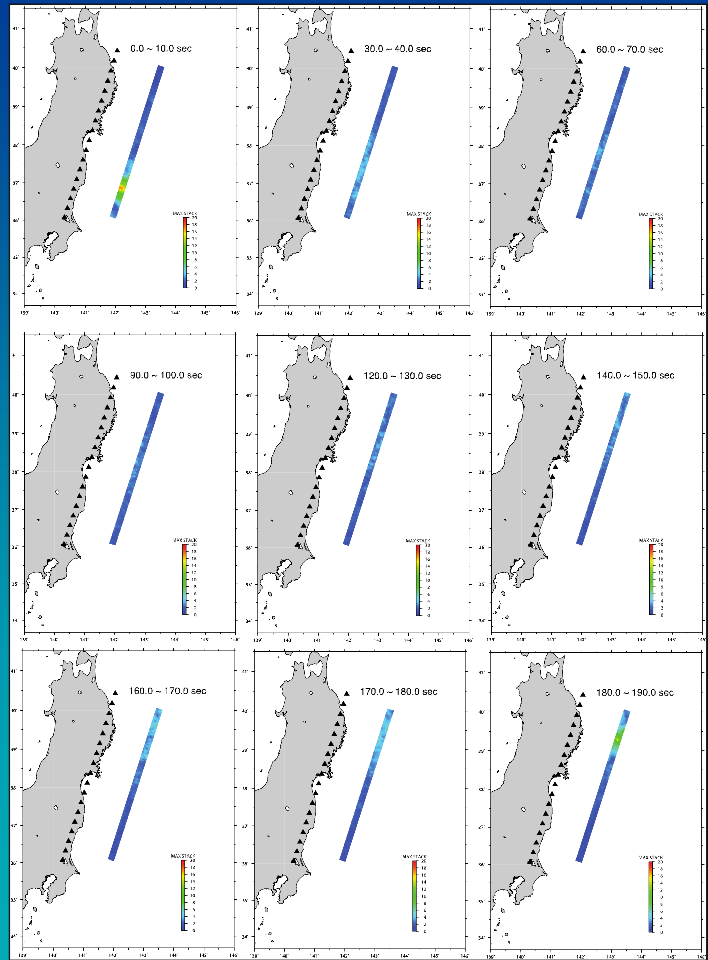

[Yano, 2012]

Single Variation in Moment Rate

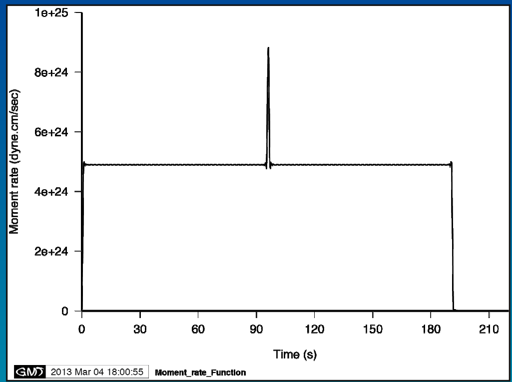

While the back projection can determine the location of the single point that varies, the amplitude is proportional only to the height above the constant moment rate. Compare beginning and ending points with the point in the middle.

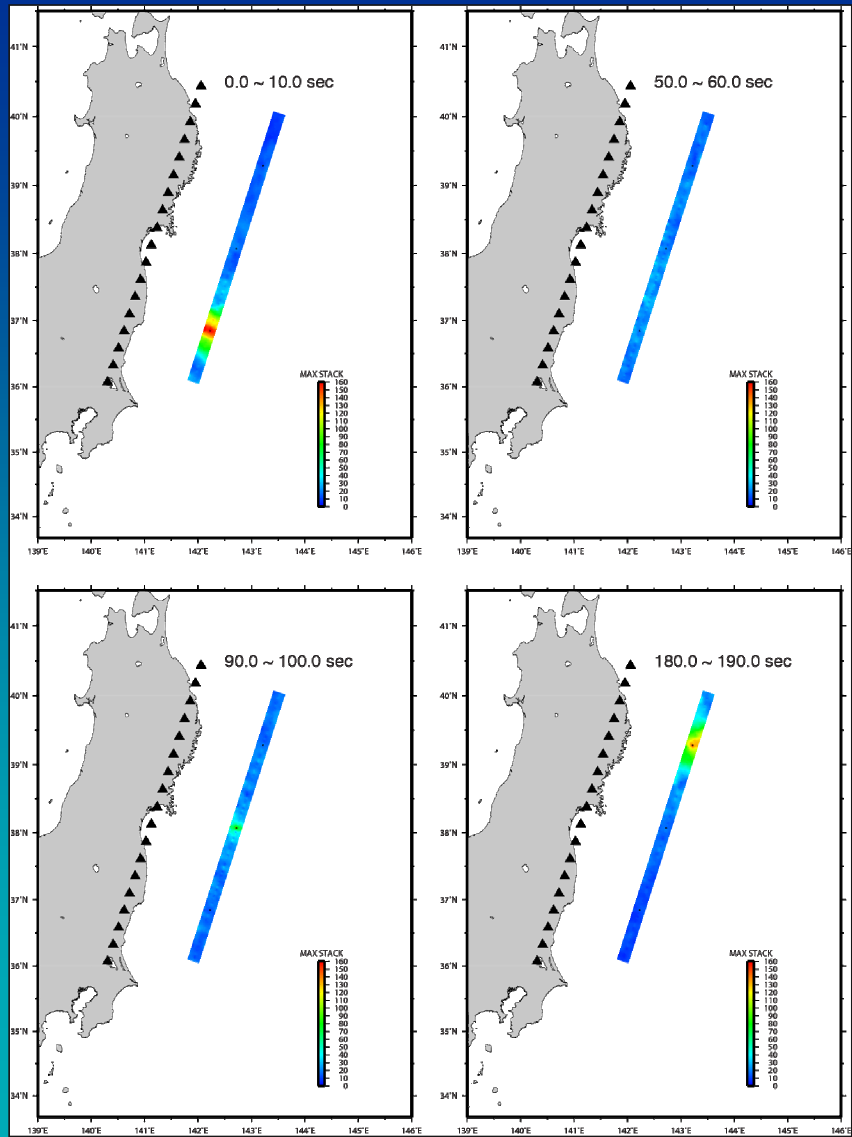

[Yano et al., in preparation]

Variation in Moment Rate

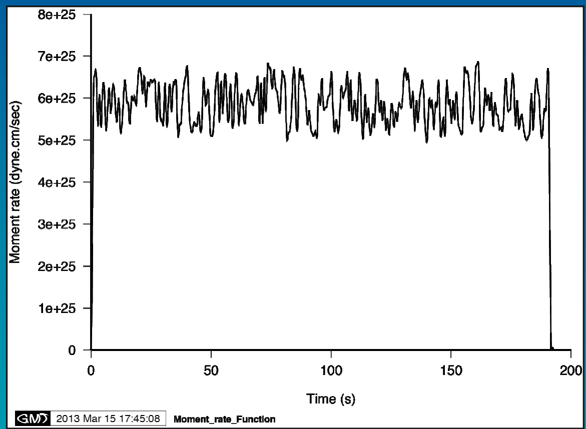

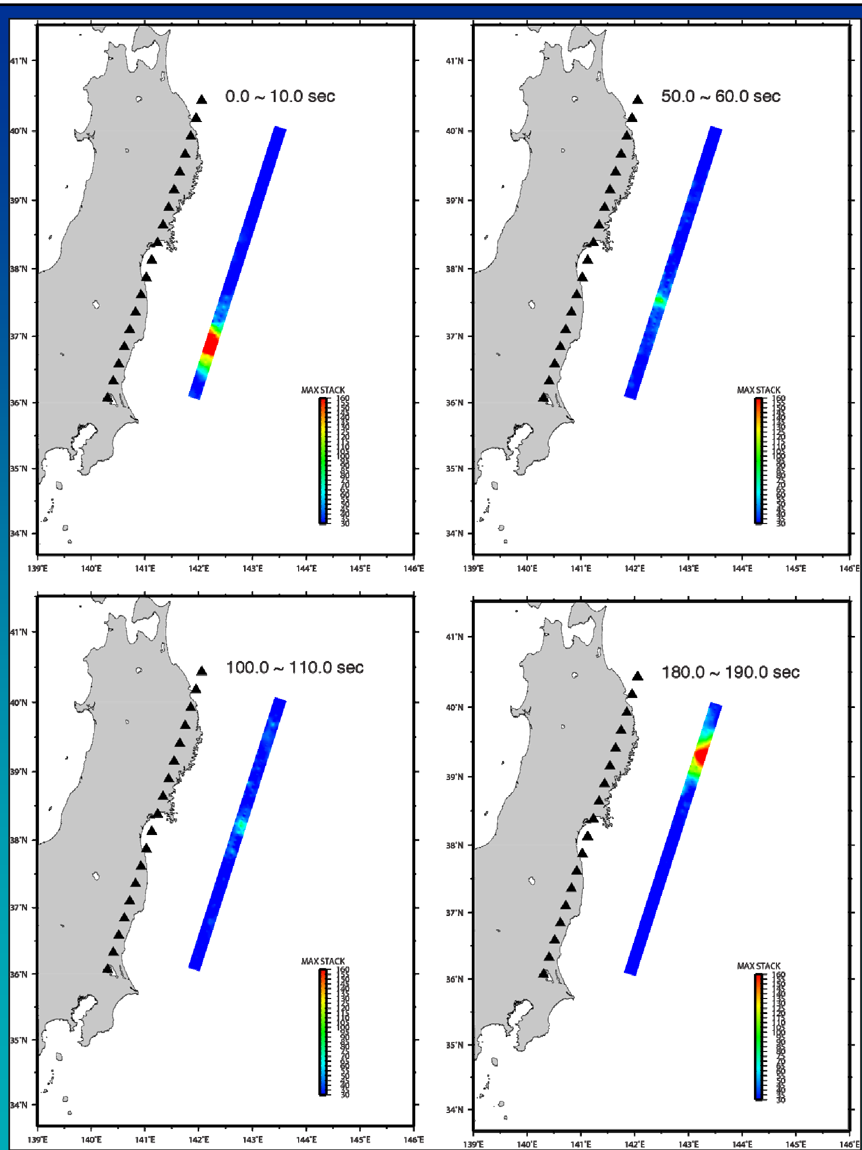

[Yano et al., in preparation]

Conclusions

- Waveform inversion may not be an effective means to determine small scale variations of the faulting.

- The variations in the moment rate function may shed light on the basic heterogeneity of the faulting.

- Back-projection analysis is good to resolve the high frequency radiation from isolated sources. But for continuous rupture, high frequency radiation captured by the back-projection analyses generally does not have a one to one relationship with the true high frequency radiation from an individual slip patch.

- The fact that rupture front of large earthquakes can be imaged by back-projection analysis implies that rupture propagation is heterogeneous.